Original Research Article

Dust outbreaks across East Iran: Application of multi-source remote sensing data (AMSR-E and FengYun3-MWRI) on the effects of soil moisture

Abstract

One of the most significant hydro-meteorological and agricultural variables is soil moisture, yet measuring it remains a difficult task. Due to the significant spatial fluctuation of soil moisture, it is difficult to quantify it in a particular spot or field across a sizable region. Despite the thermal band's limitations in assessing soil moisture, MODIS and AVHRR, which are inappropriate were utilized in this investigation. The study examined the impact of soil moisture on dust outbreak. Soil moisture in the study domain was monitored using field techniques and the hybrid model. It combined multi-sourced remote sensing data, obtained from AMSER-E and FY-3 satellites. AMSER-E satellite measures the light temperature in five frequencies ranging from 6. 9 to 89 GHz based on data obtained from AMSER-E. Findings revealed areas with a spatial scale of 25 km^2 has a 12-hour time step or variability in dust storm, thereby influencing soil moisture content within the zone of study. In addition to introducing acceptable potentials of the passive microwave band for accurate and applied monitoring of the soil moisture, the present results are viewed as a reliable source for studies on drought in time scale. The study shows that Zabol in Sistan has the highest annual average of 80.7 dust storm days. Soil moisture estimates serve a great deal for preparing soil moisture maps and the evaluation of temporal and spatial variations of soil moisture in study region to address issues related to dust storms.

Keywords: AMSER-E, soil moisture, dust, Zabol, Iran, Khorasan Razavi

1. Introduction

Dust storms are one category of major environmental issue. Dust storms are a severe meteorological phenomenon that lowers the air, reduces horizontal sight to less than 1 km, and creates a powerful, violent wind that propels small dust particles and winds from the ground. Most dust storms develop close to desert terrain. Eastern Iran's dust was flung southward, passing through several regions of the Lut plain. Sand and dust mobilization in dust-source locations has been ascribed mostly to humidity and wind speed. However, in addition to wind speed, surface characteristics also have a bearing on dust occurrences (Ravi et al., 2004; Natsagdorj et al., 2003; Wang et al., 2004; Ishizuka et al.,2005; Tegen et al., 2004; Cowie et al., 2013). Except in freezing temperatures or when there are coarse grey soils present, surface elements such as soil moisture dictate the friction threshold velocity for the release of dust in bare soil. This is due to soil moisture's amplification of the fusion forces between soil particles. Consequently, under very wet conditions, wet sand needs significant wind speed to generate a dust event. Many efforts have been made in laboratories and through observations to elucidate the mechanisms of dust emissions from moistened sand (Gillette et al., 1982; Fécan et al., 1999; Dong et al., 2002; Ravi and D'Odorico, 2005). Nevertheless, the estimation of the association between soil moisture and dust storms is only partially supported by this research. Employing satellite-based and global assimilation data would be necessary to understand the mechanisms relating dust events and soil moisture trends on a global scale and for natural dust occurrences.

One of the most significant hydro-meteorological and agricultural variables is soil moisture, yet measuring it remains a difficult task. Due to the significant spatial fluctuation of soil moisture, it is difficult to quantify it in a spot or field across a sizable region. To accurately forecast changes in the local water balance, it is crucial to assess the soil moisture, which is a crucial step in the water cycle (Salvucci et al., 2002). Due to the necessity for soil moisture to make nutrients soluble for plant absorption, spatial variations in soil moisture might vary in terms of low or varied locations in agricultural production. Due to various site-specific geology and climatic circumstances, including soil type, soil horizon, and other factors, soil moisture varies both geographically and temporally. Traditional efforts to measure soil moisture have been principally restricted to in situ measurements. High wind speeds on the ground surface promote this because soil moisture levels are directly linked to precipitation, which decreases the soil's permeability and diminishes vegetative cover (Holcombe et al., 1997). In recent years, soil moisture has been extensively monitored using microwave sensors. The accuracy of the findings received from the data is significantly influenced by the choice of the best measuring method and the most suitable band. Despite the thermal band's limitations in assessing soil moisture, MODIS and AVHRR—which are inappropriate—are used most frequently in this area of research. In view of this study which examined the impact of soil moisture on dust outbreak. Soil moisture in this study domain was monitored using field techniques and the hybrid model. It combined multi-sourced remote sensing data, obtained from AMSER-E and FY-3 satellites. This study draws attention on the usefulness of soil moisture in regulating dust storms, hence, measurement of the said component or variable either from a specific spot or across large areas remain a daunting task which calls for in-depth analyses in this regard.

2. Materials and Methods

2. 1 Description of conditions in the study region

Sistan is situated in eastern Iran, in the province of Sistan and Baluchestan's northern region (Fig. 1). Zabol City has a population of over 300,000 and is situated 215 Km from Zahedan City, the province's headquarters. Its base has recently been one of the sources of windfall deposition during droughts. Due to its geographical location, the Sistan region experiences a variety of monsoon winds, the most prominent of which is the 120-day winds, which start in late May and persist until mid-September and play a considerable role in moderating temperatures. The quaternary sediments of the Hirmand River, which are primarily of clay and sandy nature, and are intrinsically highly sensitive to wind erosion, cover the Sistan plain.

The sole naturally occurring feature in the Khajeh Mountain region of Kost Rostam is the Sistan altitudes with the north-south axis, which includes compressive folds that extend from the west to the Lut desert and from the east to the Sistan plain. The region's primary economic mainstays, agriculture and livestock, are complemented by a few rural enterprises including carpet weaving, tie and dye, petty trading and so on. Wheat, barley, cereals, as well as some fruits and vegetables, are among the crop items grown in the surrounding areas. The importance of agriculture in the area and other outlying towns is matched by the relevance of livestock breeding and animal husbandry, which are the primary activities around the Hamoon Lake.

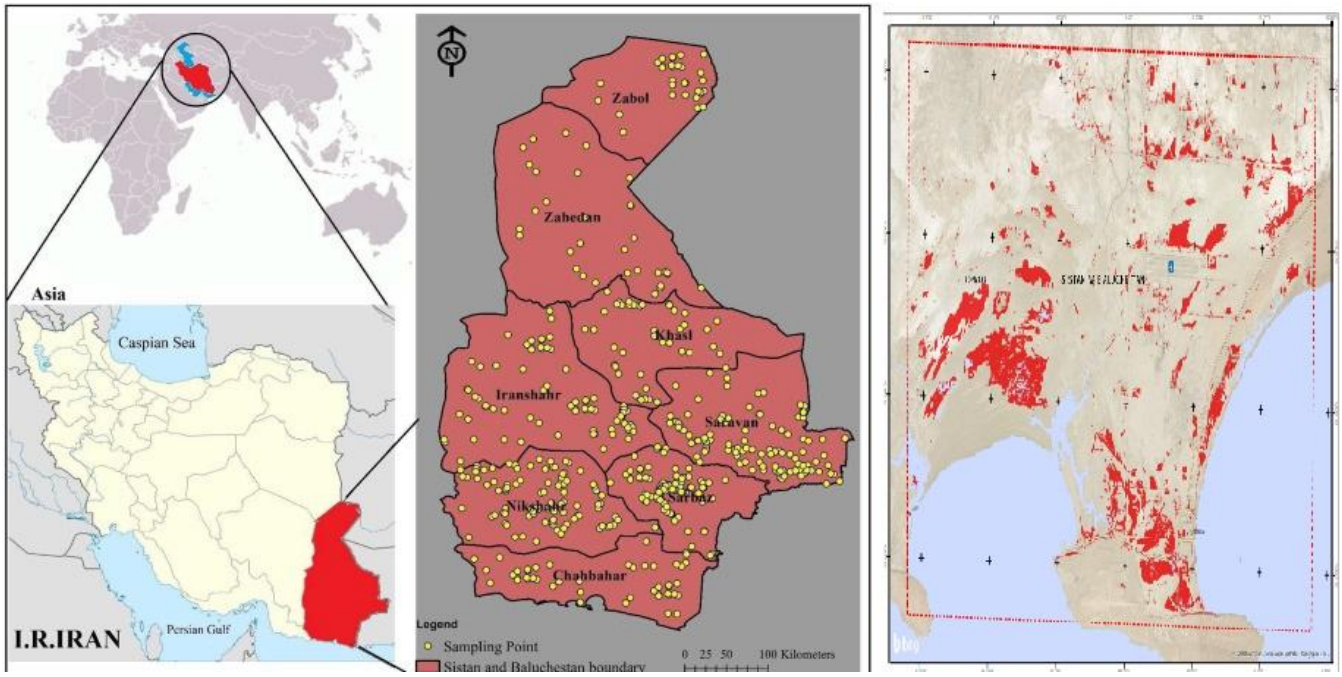

Fig. 1. The location of the study area for dust on a 3D satellite image

2.2 Datasets

Given the large amount of data from the measured variables in this study, quantitative data analysis is required to create calibration models that reflect the correlation between the dependent and independent variables, coupled with forecasting the value of the dependent variable given a set of independent variable values. The purpose of the data analysis in this research is to construct and evaluate calibration equations of the data obtained using a thermal infrared approach for the provided samples of different types of soils (clay and sand) and varying levels of compaction (compacted and non-compacted). Finding the calibration model that best captures the connection between soil moisture content and the observed variables becomes the next difficult task. Subsequently, similar expressions may be applied to precisely forecast the soil moisture content of a specific soil surface derived in a similar fashion (technique). There are several efficient calibration models, such as non-linear, linear, and polynomial models. Whilst offering equivalent predictive performance, linear models are the most commonly used and pragmatic means.

Calibration is the process of generating a model that best relates the measured dependent variable (soil moisture content) to the estimated independent variables (differential temperature (Td); relative humidity (RH); solar radiation (SR); and wind speed (WS). On the other hand, validation is the process of testing the performance of the generated model to predict soil moisture content using a new set of data called the validation data set.

The process of generating a predictive model involves the partition of the data into two portions. The first part is the calibration set. The calibration models are created using the calibration set as a training dataset. The validation set, which makes up the remaining component, is used to evaluate how well the generated model performs. Duckworth (1998) reported that using a validation set that is not used in the calibration process for testing the generated models gave the best estimate of the model's performance. This is because none of the samples in the validation set was used to develop the model. Ingleby (1999) reported that when dividing the

available data into the calibration and validation sets, it is important to ensure that they both represent the full range of possible values of the dependent variables to enhance the validity and reliability of validation testing for the entire data predictions. This can be achieved by randomizing the raw data prior to dividing them into the calibration and validation sets.

In most cases, soil moisture retrieval is performed at three different earth depth levels. Using satellite passive microwave such as AMSER-E and FY3B-MWRI satellites and ground-based observational data. Satellite data should be calibrated using field observational data. It should be considered to eliminate rainy days' data or corrupted data. That includes the following steps:

2.3 Meteorology data

Products such as wind speed (WS) at 10.0 m height, volumetric soil moisture (VSM), and soil temperature at a depth of 0–10.0 cm, and rainfall rate will be used from meteorology stations. There are more than 100 meteorological stations which are primarily automatic and synoptic in the study area.

Table 1: Some synoptic meteorological stations in the study area.

Station name	*Latitudes*	*Longitudes*
Fariman	35.278318	59.609543
Ghochan	37.215004	58.308025
Golmakan	36.240662	59.088936
Gonabad	34.091207	58.308025
Kashmar	35.039524	58.308025
Khaf	34.327277	60.13015
Mashhad	36.240662	59.609543
Nyshabour	36.240662	58.308025
Sabzevar	36.240662	57.26681
Sarahks	36.240662	61.171365
Torbate hey	35.278318	59.088936
Torbate Jam	35.039524	60.390454

2.3.1 Soil Moisture Data Preprocessing

Significant differences were observed in the data collected for the soil moisture content from different units. P-value (0.769) was found using the Dixon's test and was more than the significance level of 0.05 alpha, allowing soil moisture data to be taken into account without flood data. Atmospheric and geometric corrections for FY-3 images were performed. Regarding the smoothness (at least 1214 and maximum 1500 meters above sea level) and the lack of high topographic conditions in the study area, the ATCOR2 model was used as the absolute atmospheric correction (for geometric corrections of ground-corrected reflecting data from Google data). In this investigation, the inheritance was employed, and the desired root means square error was 0.622 pixels. By comparing it to GPS data and doing geometric adjustments on mid-scale imagery like Thematic Mapper, Google Earth data shows that the square root mean square deviation of 0.00014 is accurate.

2.3.2 AMSER-E satellite imagery

In this study, the data obtained from AMSR-E- EOS of NASA were utilized. Products of the soil moisture have been elicited from AMSR-E/Aqua Daily L3 Surface Soil Moisture, Interpretive Parameters, & QC EASE-Grids ascending and describing data. This series of images has been prepared for a 1-year statistical period (Since the beginning of January 2009 until the beginning of January 2010) at a spatial resolution of 25 Km^2 and a 12-hour time step. AMSR-E on NASA's EOS Aqua satellite was launched on May 4 2002, and had operated until October 4 2011.

As the successor to AMSR-E, AMSR2 on-board the sun-synchronous satellite GCOM-W1 was launched on 18 May 2012 by JAXA. GCOM-W1 is the first of three planned satellites of the GCOM-W project, which is a 13-year mission designed for global and continuous observation of Earth's water and energy cycles. AMSR2 has most of the characteristics of AMSR-E. Both sensors are conical scanning passive microwave radiometers with similar instrument configurations. The AMSR instruments measure microwave emissions from the earth surface twice daily for descending/ascending orbital equatorial crossings at 1:30 AM/PM local time, with vertically (V) and horizontally (H) polarized Tb retrievals at six frequencies (6.9, 10.7, 18.7, 23.8, 36.5, 89.0 GHz). Major changes in AMSR2, distinctive from AMSR-E, include an additional frequency at 7.3 GHz designed for mitigating Radio Frequency Interference (RFI), and a larger (2.0 m diameter) main reflector for enhanced spatial resolution. The MWRI onboard the FY-3B satellite was launched 5 November 2010. Similar to the channel setting and view geometry of AMSR-E, MWRI conically scans the Earth at five frequencies (10.7, 18.7, 23.8, 36.5, 89.0 GHz) and dual (H, V) polarizations. The MWRI has four major differences considering AMSR instruments, including: (a) no C-band channel relative to the AMSR 10.7 GHz channels due to widespread C-band RFI; (b) coarser spatial resolution and slightly narrower orbital swath for all frequencies relative to the AMSR sensors; (c) an approximate 10-min satellite overpass time difference between MWRI and AMSR-E; and (d) an approximate 53-degree earth incident angle (EIA) of measurement instead of 55 degrees for the AMSR sensors. Detailed sensor configurations for AMSR-E, AMSR2 and MWRI are summarized in Table 2.

Table 2: Satellite microwave sensor configurations used in this study

	Instrument configurations		
Specifications	AMSER-2	AMSER-E	MWRI
Satellite Platform Time (Local time zone)	GCOM-W1 1:30 p.m. Ascending 1:30 a.m. Descending	AQUA 1:30 p.m. Ascending 1:30 a.m. Descending	FY3B 1:40 p.m. Ascending 1:40 a.m. Descending
Antenna Size	2 m (Diameter)	1.6 m (Diameter)	0.977 m × 0.897 m
incident angle	55	55	53
	Spatial Resolution (km×km)		
Band (GHz)	AMSER-2	AMSER-E	MWRI
6.93	62 × 35	75 × 43	N/A
7.3	62 × 35	N/A	N/A
10.65	42 × 24	51 × 29	85 × 51
18.7	22 × 14	27 × 16	50 × 30

23.8	19 × 11	32 ×18	45 × 27
36.5	12 × 7	14 × 8	30 × 18
89	5 × 3	6 × 4	15 × 9

2.3.3 FY3B-MWRI satellite Images

The FY3 series MWHS is a five-channel cross-track scanning instrument able to provide vertical humidity information to the NWP data assimilation systems. The vertical resolution is poor, with only 2 to 3 pieces of independent information. Nonetheless, this has been proven valuable to NWP in the past.

2.3.4 Soil moisture retrieval using satellite images

The satellite images offer brightness temperature and soil moisture that is affected by vegetation and soil type. Analyzing field survey data and satellite images using regression methods helps to calibrate satellite data. Various algorithms for retrieval of soil moisture from radiometer brightness temperature have been developed, including single channel algorithm (SCA), land parameter retrieval model (LPRM), physically based statistical methodology (PBSM)18, and official algorithms developed by national aeronautics and space administration (NASA) of the United States and Japan aerospace exploration agency (JAXA) according to AMSR-E configurations. All these algorithms are based on the same radioactive transfer model. (Omega-tau) which assumes that vegetation multiple scattering and reflection at the air-vegetation interface are negligible. The SCA is basic option for the Chinese FY-3 soil moisture products. Meteorological data such as wind, horizontal visibility, field observation and precipitation data will be used to retrieve Dust storm occurrence and severity.

2.3.5 Satellite image processing

Before using satellite images, the following corrections (Fig. 2) are applicable to the understudied data, depending on some key parameters.

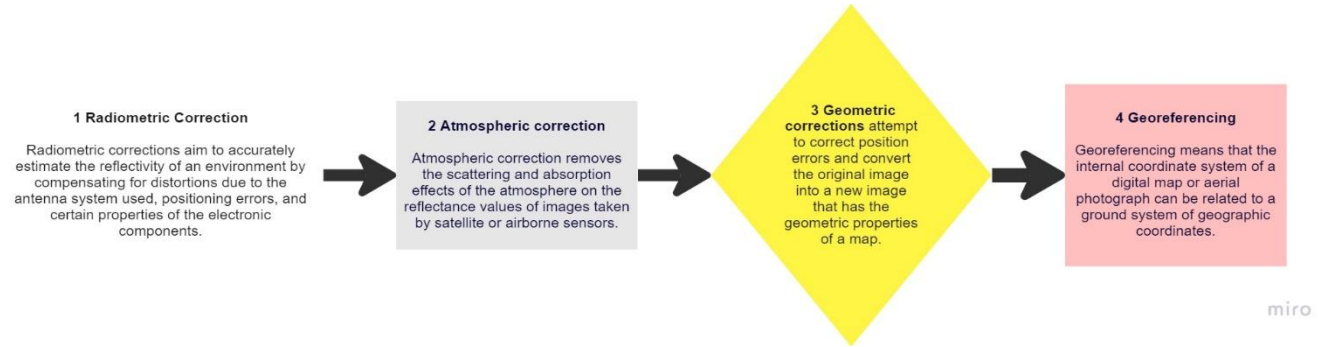

Fig. 2. Conceptual flow of satellite image corrections.

1. Radiometric correction 2. Atmospheric correction 3. Geometric correction 4. Georeferencing

2.3.6 Radiometric correction

Radiometric errors depend on the physical properties of the sensor. Over time, the radiometer will be amortized and, as a result, the sensor will be affected by errors such as distance from the sun, the change in the angle of zenith, and so on, radiometric corrections must be made on the images to resolve these errors. For this

purpose, the first step is the conversion of numerical values (DN) to spectral radiation, which is performed using the calibration coefficients of the sensor, and then the amount of spectral radiation calculated is converted into spectral reflection.

$$\% \text{ Albedo} = (A * DN) + B \cdots (1)$$

Here, DN is the pixel digital value and A and B are the calibration coefficients of the satellite.

Atmospheric correction involves removing noise in this case clouds and aerial distortions from the images and obtaining reflections from the surface of the earth whiles Geometric corrections eliminates the spatial-spatial errors caused by pixels, the factors causing these errors, the curvature of the earth, the imaging state, the type of satellite view, the post and the heights of the ground, height and speed of the sensor.

AMSR-E / Aqua Daily L3 Surface Soil Moisture, Interpretive Parameters, and QC EASE-Grids are combined and soil moisture is globally and in terms of obtained. Then, these data were geo-reference and soil moisture was extracted in Iran and by Khorasan Razavi province for 2009.

2.4 Data Analysis

2.4.1 Comparison of the degree of soil brightness in dry and wet conditions:

The amount of energy received by the sensor, which determine by the brightness (DN) of the images, is converted to the brightness temperature using the inverse of the Planck function and based on the following relationships. Figures (3) and (4) shows difference in the brightness of the DN4-DN5 bands and the brightness of the bands of the BT4-BT5 bands show quite dry and perfectly wet conditions after atmospheric conditions.

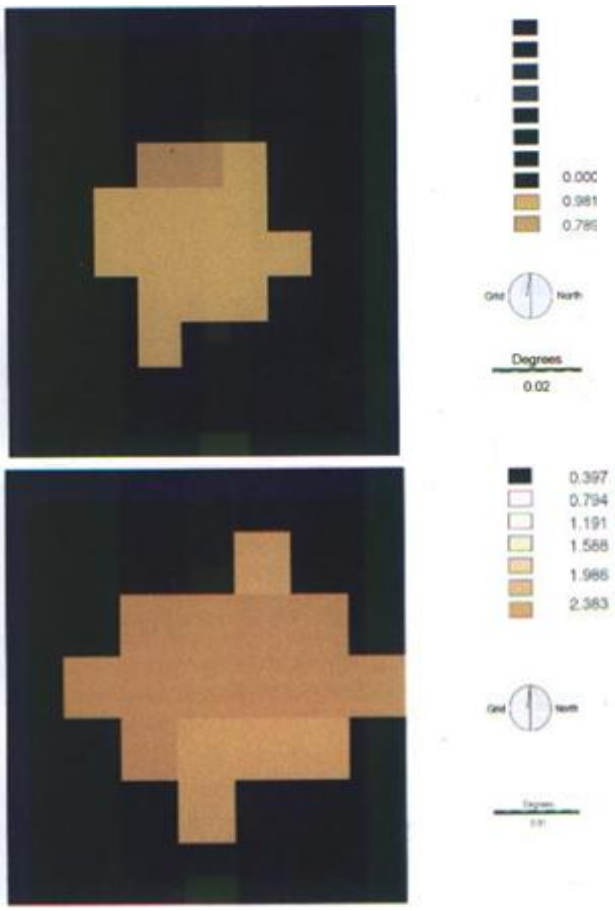

Fig. 3. Differences between degrees of lighting in wet and dry soil- DN4-DN5 bands

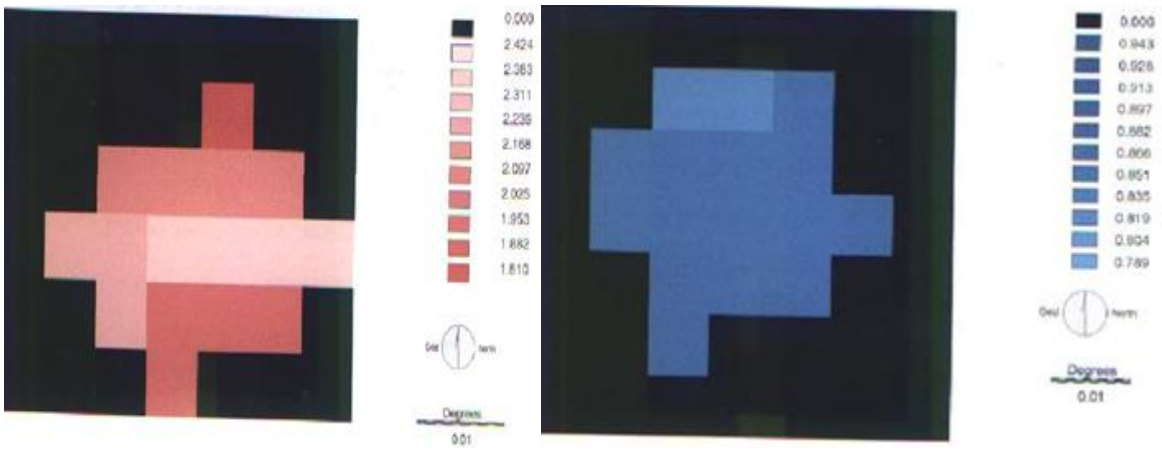

Fig. 4. Differences in thermal band (BT4-BT5) temperatures in wet and dry conditions

As it is seen, the values obtained from the soil surface in dry soil conditions range from (-5 to -13), whereas that of humid conditions range from (8 to 10).

2.4.2 Quantity of albedo in different humidity conditions using reflective bands

Soil texture in the study area is determined using the global database, the amount of albedo has been determined in different conditions, and the final calibrated results have been determined. An example of the calibration coefficients presented in the global database of NOAA:

Table 3: Bands, slope and intercepts.

Band	SLOPE	INTERCEPT
b_1	0/1081	-3/8648
b_2	0/1090	-3/6749

$$B1 = -\frac{3}{8648} + \frac{0}{1080} - b_1 \dots (2)$$

$$B2 = -\frac{3}{6749} + \frac{0}{1090}\ b_2 \dots (3)$$

Based on the above relations, the amount of albedo in each pixel, such as the ground, it calculated according to the different soil moisture conditions, and then the average albedo obtained is determined as the desired pixel albedo.

2.4.3 Estimation of moisture content for soil surface layer (in grams per cubic centimeter)

In order to estimate the surface soil moisture, brightness temperature, the surface temperature, the albedo of each image pixel and its equivalent were calculated in the specified period. The obtained data were in grams per cubic centimeter changed to volume unit (percent) to be analyzed. The soil moisture content defined as the ratio of the water weight in the soil mass to the weight of its solid components (Abshoori, 1377). We had two scans for every point per day for a 12-hour interval. One scan was randomly selected. There have been 360 scans in one year for the entire area under study (Khorasan Razavi province).

To convert mass moisture to volumetric moisture, it is required to have the particle density of the soil in that region per cubic centimeter. The soil particle density is defined as the weight of soil in a given volume

(g/cm3) (Nouroozi et al. 1387). The space between particles is not associated with the particle density. The particle density of the soil ranges from 2.60 to 2.75 g/cm^3. This value is almost constant, since most of the minerals existing in the soil have the similar density. The soil density exceeds 2.75 in the presence of such mineral's tourmaline, magnetite and hornblende. Organic materials are lighter than minerals. Therefore, soils that contain relatively large amounts of organic matter have lower particle density, and according to this principle, the particle density of surface soil is always lower than that of the soil below the surface of the ground.

$$D' = \left(\frac{P'}{V'}\right) \dots (4)$$

D: Bulk density in g/cm^3

V': Volume of dried soil in 105 ° C in a normal condition in terms of cm^3

P': Weight of dry soil in 105 ° C in a normal condition in terms of g.

According to the particle and bulk density of the soil and by using the following formula, the soil porosity is calculated:

$$The\ soil\ porosity = 100 - (particle\ density|bulk\ density)\ \times 100 \dots (5)$$

The soil must have appropriate porosity for water and aeration. The percentage of soil volume occupied by solid matters is equal to the ratio of bulk density to particle density, multiplied by 100.

Finally, it is necessary to mention that new information sources and optimized methods have been effective in estimating and measuring surface soil moisture. One of these methods is use of AMSER-E, which provides processing, and correction of the data, extraction and evaluation of such indexes as soil temperature, brightness temperature by using separate bands and the soil surface albedo through performance of difference steps.

3. Results

3.1 Dust Density in 2014

The dust intensity map (Fig. 5) is a product that has been generated by applying a dust monitoring and processing model of over 2053 MODIS satellite imagery with a resolution of 10 km in 2014 (daily). This monthly average map shows the intensity of the dust in each area. Also, due to the comparison of the results with ground stations, the values of the intensity above the chosen threshold represent the phenomenon of dust and, as much as it is added, the phenomenon of dust in the region will be more severe.

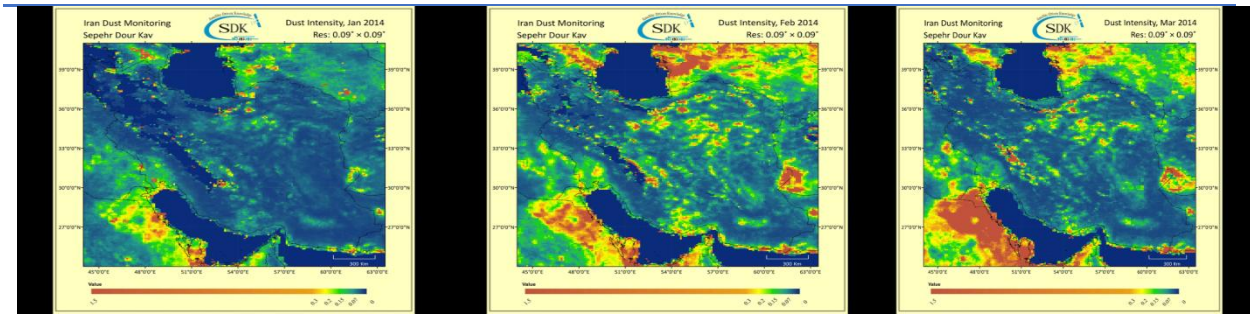

JAN 2014	FEB 2014	MARCH 2014

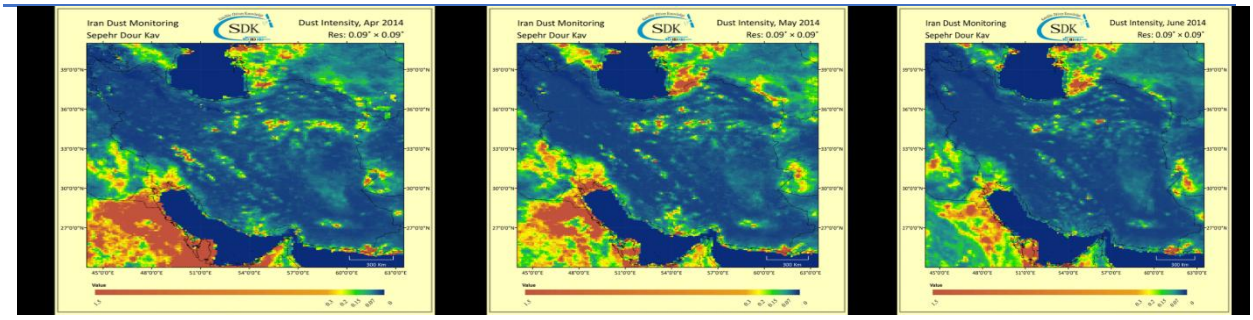

APR 2014	MAY 2014	JUN 2014

Fig. 5. 2014 Dust density maps of the study domain

3.2 Dust intensity for 2017

The dust intensity map is a product that has been generated by applying a dust monitoring model and processing more than 979 MODIS satellite imagery with a resolution of 10 km in 2017 (on a daily basis). This monthly average map shows the intensity of the dust in each area (Fig. 6). Also, due to the comparison of the results with ground stations, the values of the intensity above the chosen threshold represent the phenomenon of dust and, as much as it is added, the phenomenon of dust in the region will be more severe.

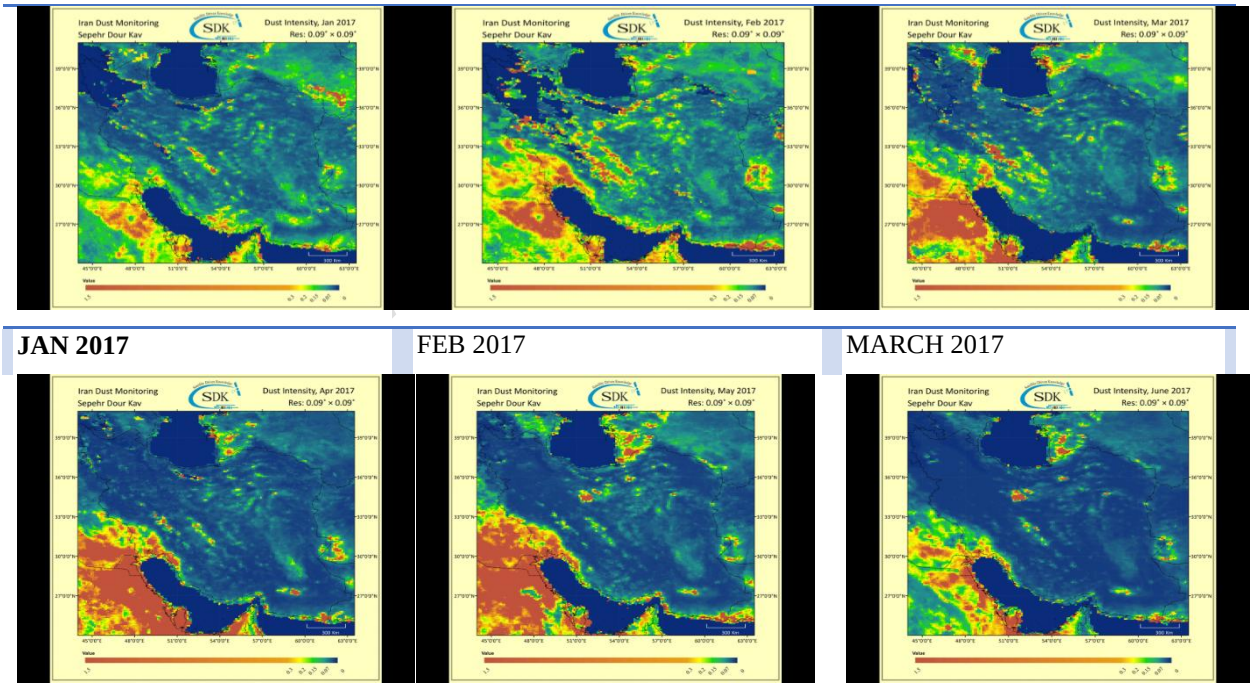

JAN 2017	FEB 2017	MARCH 2017
APR 2017	MAY 2017	JUN 2017

Fig. 6. 2017 dust density maps

3.3 Investigation of soil moisture changes in relation to dust storms.

At this stage, we plan to investigate the changes in soil moisture in the dates of the occurrence of dust. Therefore, we will draw up the moisture maps for the last few days and then examine the process of change.

Table 4: Major dust storm events in the study area

Relevant dates	Type of phenomenon	Place of occurrence
June 22 to July 3, 2017	Dust storm	Sistan and Baluchestan province
26 to 29 April 2017	Dust storm	Sistan and Baluchestan province
30 September to 4 October 2016	Dust storm	Khuzestan

3.4 Land surface soil moisture maps for 2017

Figure 7 shows the land surface's soil moisture for the given study period; thus, between June 22 and July 3, 2017.

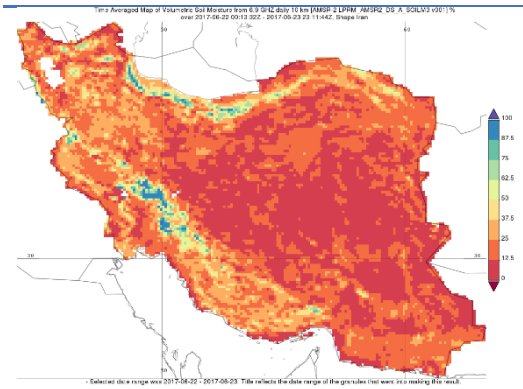

22-Jun-2017-Ascending

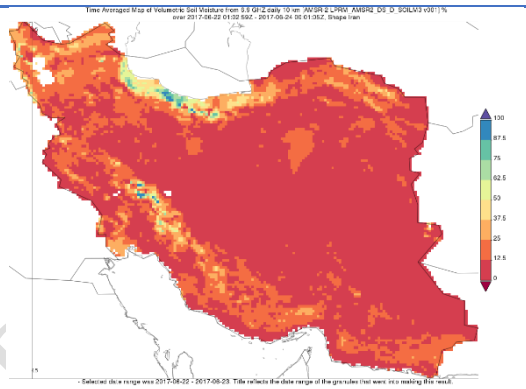

Descending-22-Jun-2017

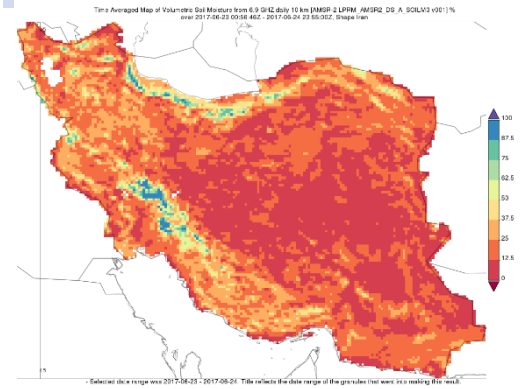

23-Jun-2017-Ascending

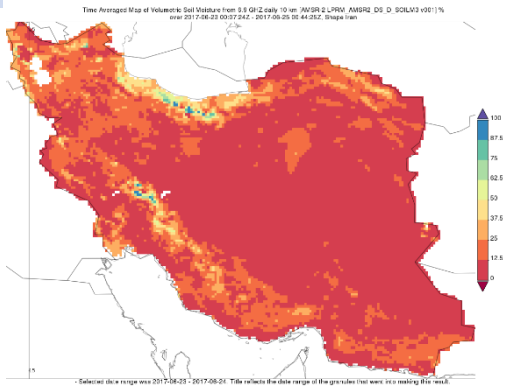

Descending-23-Jun-2017

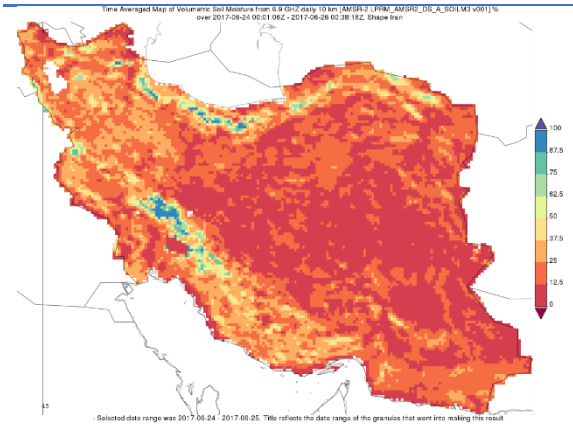

24-Jun-2017-Ascending

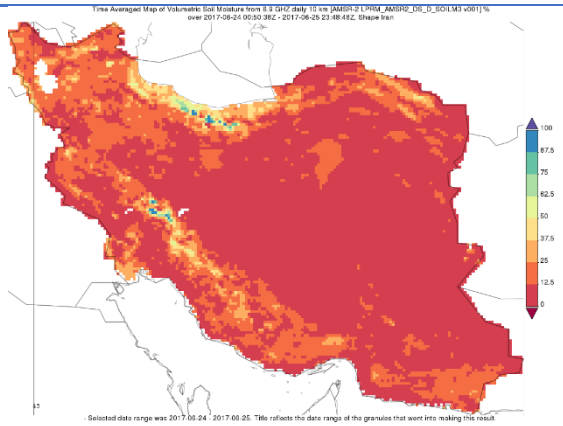

Descending-24-Jun-2017

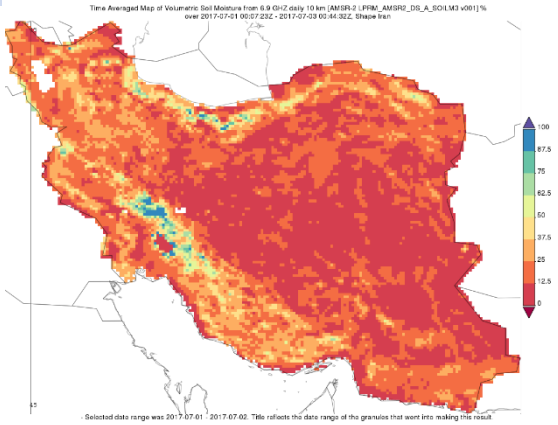

01-July-2017-Ascending

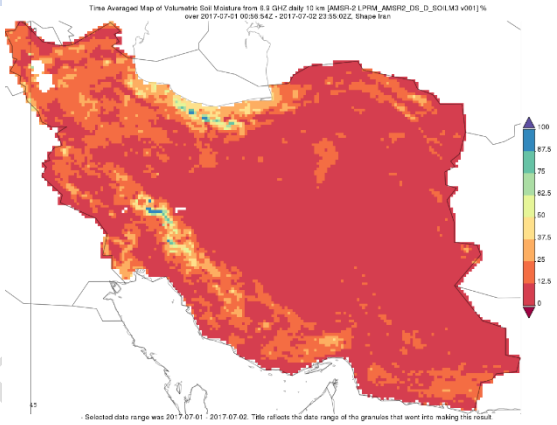

Descending-01-July-2017

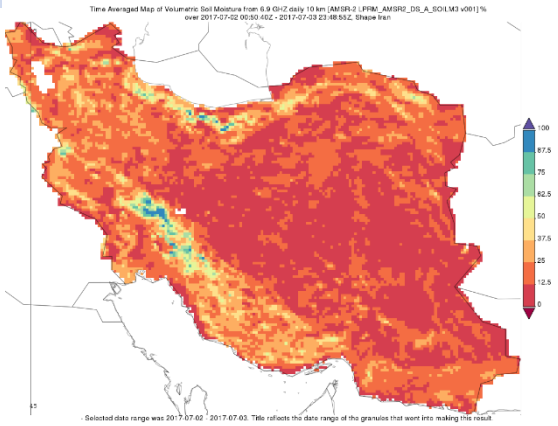

02-July-2017-Ascending

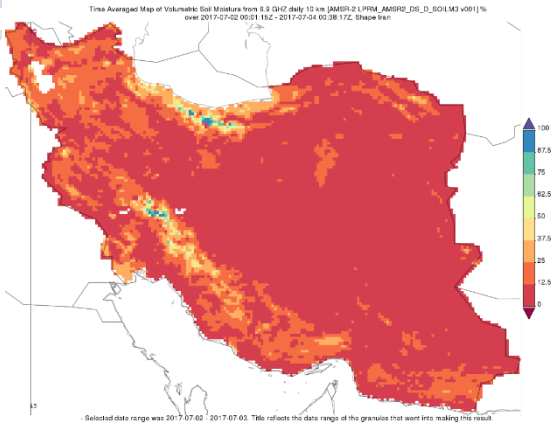

Descending-02-July-2017

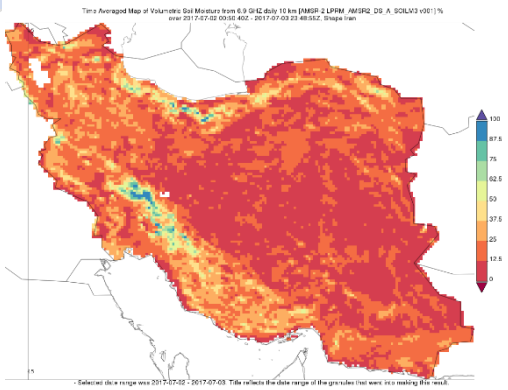

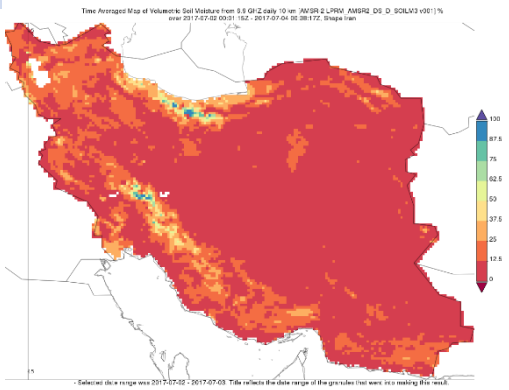

03-July-2017-Ascending	**Descending-03-July-2017**

Fig. 7. Time averaged map of soil moisture from 6.9GHZ daily 10 km (AMSER-2)-IRAN

3.5. Parametric monitoring of dust events

The combination of wind parameters and soil moisture has a great influence on the formation of dust in a particular region. In this way, as the amount of soil moisture decreases and the wind speed increases, the probability of a dust phenomenon also increases. This problem is more common in areas with poor vegetation than in other areas. The following figures show the state of soil moisture and the intensity of daily dust in the Sistan and Baluchestan region of southeastern Iran, and the graph shows the status of wind speed, soil moisture and dustiness or absence of specific days from 2015, 2016 and 2017 (Figs. 8 and 9). Comparing the situation on 23/04/2016 and 07/04/2017, or 12/06/2016 and 16/09/2016, it can be concluded that at the same wind speed, an increase in the percentage of soil moisture can be due to the occurrence of the event prevents dust. Therefore, the long-term correlation between these two parameters with the occurrence of dust storms can be found in extracting the threshold limits of these variables to create dust storms.

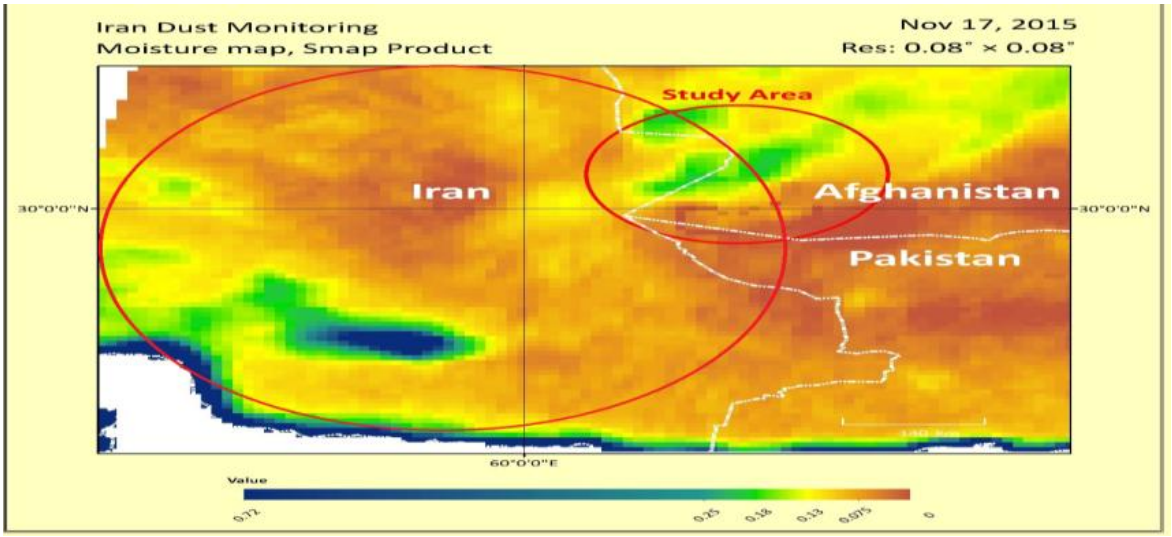

Fig. 8. Soil moisture map extracted from SMAP images with a resolution of 9km - The small red circle indicates the origin of the dust and the studied area.

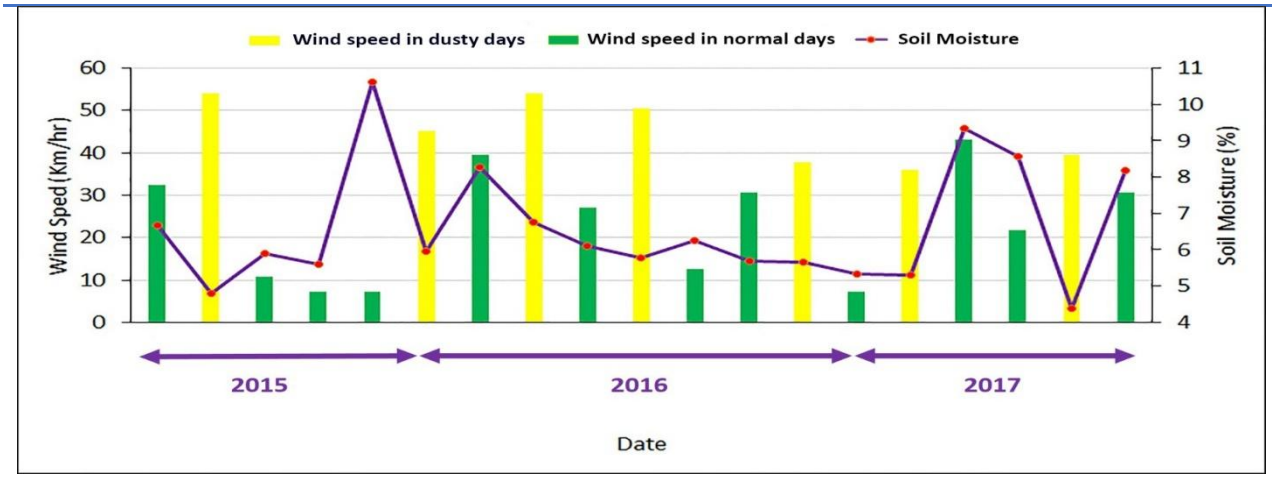

Fig. 9. Wind speed and soil moisture diagram

Combination of wind speed and soil moisture diagram - yellow diagram showing the events of the dust and the green diagram indicating the days without dust - Increasing the moisture content of the wind with the same wind speed, in most cases preventing the storm of dust.

3.6 The relationship between soil moisture content and dust concentration

Table 5 shows the amount of soil surface moisture content and the density of the dust in the understudied areas.

Table 5: Amounts of soil surface moisture content and the density of the dust of the studied areas

RH	50.0	39.0	28.0	17.0	15.0	13.8	12.6	11.4	10.2	9.0	7.8	6.6	6.0
density	40	45	50	55	60	65	70	75	80	85	90	95	100
5.9	5.6	5.4	5.2	4.2	3.2	2.1	1.1	1.0	0.9	0.9	0.8	0.7	0.7
105	110	115	120	125	130	135	140	145	150	155	160	165	170

Table 5 shows the relationship between soil surface moisture content and the density of the dust of the studied areas. As is clear, the concentration of released dust on the soil surface has decreased with increasing relative humidity. Detection of the rate of decline for different regions of the soil is different, but all soils have fallen sharply in humidity by 2.2% and are approaching zero.

Therefore, we can say that at a humidity point of 2.2%, inter-particle forces have the greatest effect on the moisture content of the surface soil to increase adhesion between soil particles.

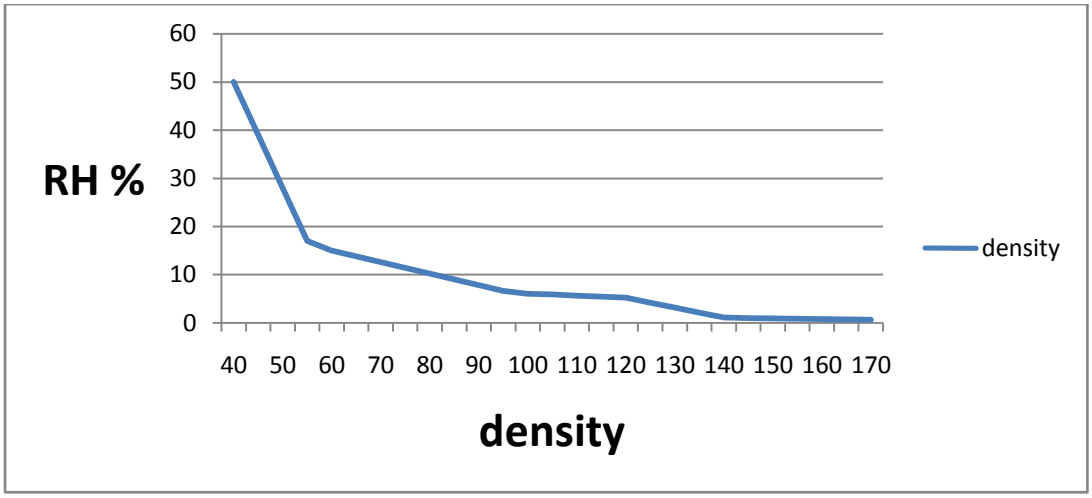

Fig. 10. The relationship between soil moisture content and dust concentration

Evidence presented above (Fig. 10) indicates dry soil (humidity near zero) has the highest dust production rate of 168.66 mg / m3. This amount is more than 1000 times the standard human standard (150 mg / m^3). With increasing humidity from zero to about 3%, the amount of dust released has dropped.

3.7 Validation of Error Estimation of Satellite Soil Moisture

In order to study the accuracy of soil moisture retrievals in the study areas, soil moisture data of AMSER-E and FY-3 and ground data (weather stations) were evaluated using various statistical indices. In order to verify the surface moisture content obtained from the microwave data, the correlation of Zabol and Zahedan cities with surface moisture content obtained in two AMSER-E and FY-3 satellites was investigated. Table 6 clearly shows correlation coefficient of surface moisture content obtained on AMSER-E satellite of Zabol and Zahedan cities.

Table 6: Correlation coefficient of Zabol and Zahedan cities against surface moisture content

	ZABOL			ZHAHEDAN		
Year	The correlation coefficient	90% level	95% level	The correlation coefficient	90% level	95% level
2013	0.363	*	*	0.517	*	*
2014	0.460	*	*	0.204	-	-
2015	0.509	*	*	0.330	*	*
2016	0.330	*	*	0.296	*	*
2017	0.688	*	*	0.431	*	*

Table 7 clearly shows correlation coefficient of surface moisture content obtained on FY-3 satellite of Zabol and Zahedan cities.

Table 7: Correlation coefficient of Zabol and Zahedan cities against surface moisture content

	ZABOL	ZHAHEDAN

Year	The correlation coefficient	90% level	95% level	The correlation coefficient	90% level	95% level
2013	0.606	*	*	0.738	*	*
2014	0.821	*	*	0.78	*	*
2015	0.561	*	*	0.744	*	*
2016	0.734	*	*	0.419	-	-
2017	0.51	*	-	0.746	*	*

In this section, the correlation of humidity between Zahedan and Zabol stations was investigated with surface moisture content obtained from the E-AMSR and FY-3 sensors. The results show a significant correlation between surface and satellite surface moisture at 90% and 95% confidence levels.

Correlation coefficient in AMSER-E satellite is not significant only at Zahedan station in 2014 and correlation coefficient at Zahedan station in 2016 and at Zabol station in 2017 is not significant at 95% level. This correlation between surface and surface water content data shows the adequacy of these data and confirms the usefulness of using such wide area coverage data in water and soil research.

4. Discussion

Soil moisture quantification across the entire region, is known to be one of the most challenging environmental indices which has been observed to be very important, yet difficult to quantify. In establishing the various findings of this study, the MODIS data points out that there is generally severe dust in this region of study. Monthly average dust observations of 2014 through to 2017 depict high dust over the area (Pour Kermani, 1365). Table 4 shows the major dust event dates between some specific wind parameters and soil moisture. These parameters have great influence on the formation of dust in the study domain. Findings revealed as the amount of soil moisture decreases, whilst the wind speed increases, the probability of a dust phenomenon also increases as revealed by (Salvucci et al., 2002). This could be attributed to the poor vegetation of the area. In 2017, as shown in Fig. 7., soil moisture varied from 6.9GHZ daily with every 10 km using the (AMSER-2) in southeastern Iran.

Correlation analysis between wind speed and soil moisture is displayed in Fig. 9. Based on evidence presented in Fig. 9, an inverse relationship between wind speed and soil moisture between 2015 and 2017 period could be observed. Here, increasing moisture content of the wind along the speed of the wind prevents the formation of dust storms and this is clearly confirmed by (Holcombe et al., 1997). Over the study period, the three different months studied revealed precipitation varied; thus, 30mm, 6mm and 4 mm in 2015, 2016 and 2017 respectively. Table 5 presents the relationship between soil surface moisture content and the density of dust in the study region. The concentration of released dust on the surface of the soil has decreased with increasing relative humidity. Detection of the rate of decline for different regions varies; however, results prove all the soils have sharply reduced in relation to humidity by 2.2%, approaching the zero margins.

Moreso, we further validated the error estimation of the satellite's soil moisture. Tables 6 and 7 shows the correlation of humidity between Zahedan and Zabol ground-based stations and satellites. These were investigated using surface moisture content obtained from the E-AMSR and FY-3 sensors. The results show a significant correlation between surface and satellite surface moisture at 90% and 95% confidence levels (Ravi et al., 2004; Natsagdorj et al., 2003; Wang et al., 2004; Ishizuka et al., 2005; Tegen et al., 2004; Cowie et al., 2013). Based on these findings, we can conclude that there was a strong correlation between soil moisture content as measured by AMSR-E and rainfall data in the study area. Correlation coefficient in AMSER-E satellite was insignificant at Zahedan station in 2014. Again, the correlation coefficient of Zahedan station in 2016, and that of Zabol station in 2017 was also not significant at 95% confidence level. The association of surface and surface water content data shows the adequacy of these datasets, which confirms the usefulness of using such wide area coverage data in water and soil research.

The varying nature of soil moisture makes it a daunting task in quantifying it in a spot or field across a sizable region in hydrological and climatological studies. MODIS and AVHRR datasets which were plainly tagged as inappropriate for such measurements or studies of this nature were used. Additionally, the datasets used which encapsulated minor errors were scaled or normalized to enhance the study's validity and reliability in drawing logical conclusions. Further studies could consider technological developments or strategies for accurate recording of data and measurements of discrepancies in soil moisture measurements, as shown in the present study that soil moisture despite its environmental relevance varies across space.

5. Conclusion

The accuracy assessment and accuracy of surface soil moisture data at large spatial scales is essential for careful and accurate environmental surveys. Now we can conclude that direct measurement of soil moisture and the extraction of moisture data in a point is not only costly and time-consuming, but on a large scale, it is not practical. Despite the importance of soil moisture in environmental studies, due to the cost and time consuming of spot measurements, this parameter is not widely used in climatic models. Due to the lack of availability of long-term soil moisture data at Iran's meteorological stations, microwave satellite data is used due to its continuous measurements of the surface of the earth, ability to record physical properties of different coatings on the ground and long-term archives are a good substitute for soil moisture spot measurements. By using satellite data, it is possible to prepare time and spatial distribution of relative humidity of soil in networks ranging from 500 m to 20 km depending on the type of sensor. Among the key highlights or relevance of this research is that, when considering the capabilities of the AQUA satellite for measuring soil moisture and its adaptation to the climatic realities of Iran, the moisture content extracted from the satellite and the precipitation status of Khorasan province in the understudied stations were checked to ensure that the AMSER and FY-3 satellite data have high accuracy.

Therefore, it is possible to use the data of these satellites to evaluate drought monitoring, hydrology, weather and forecasting of storm and dust. Similarly, its applicability is essential in the agriculture and natural resource management sectors for modelling and soil moisture assessment purposes. Overall, it can be concluded that soil moisture retrievals are well-matched in comparison to the measured data at study stations. Lack of soil moisture data in most parts of Iran is always a major problem in hydrological modeling, meteorological

forecasting and water resource management and planning. Therefore, based on the results of this study, soil moisture estimates can serve as a suitable tool for preparing soil moisture maps and the evaluation of temporal and spatial variations of soil moisture in study region to address issues related to dust storms.

Data Availability

The data that backs up the study's conclusions is accessible and will be supplied upon request.

References

Akbari, M., Toomanian, N., Droogers, P., Bastiaanssen, W., and Gieske, A., (2007), Monitoring irrigation performance in Esfahan, Iran, using NOAA

De Ridder, K., (2000), Quantitative estimate of skin soil moisture with the Special Sensor Microwave/Imager. Boundary-Layer Meteorol, 96: 421-432.

Draper, C., Walker, J., Steinle, P., de Jeu, R. and Holmes, T., (2009)."*An evaluation of AMSR–E derived soil moisture over Australia*", Remote Sensing of Environment, 113 (4), 703-710.

Marshall, G.S., (2005), Drought Detection and Quantification Using Field-Based Spectral Measurements Of Vegetation In Semi-Arid Regions. New Mexico Institute of Mining and Technology Department of Earth and Environmental Science.

Mattia, F., Satalino, G., Pauwels, V.R.N., and Loew A., (2008), Soil moisture retrieval through a merging of multi-temporal L-band SAR data and hydrologic modeling. Hydrology and Earth System Sciences, 5: 3479–3515.

Moran, M.S., Peters-Lidard, C.D., Watts, J.M., and McElroy, S., (2004), Estimating soil moisture at the watershed scale with satellite-based radar and land surface models, Can. J. Remote Sens.,.

Narasimhan, B., and Srinivasan, R., (2005), Development and evaluation of Soil Moisture Deficit Index (SMDI) and Evapotranspiration Deficit Index (ETDI) for agricultural drought monitoring. Agricultural and Forest Meteorology, 133: 69–88.

Palmer,W.C., (1965), Meteorological Drought. Research Paper No. 45, US Weather Bureau, Washington, DC.

Peñuelas, J., Piñol, J., Ogaya, R., and Filella, I. (1997), Estimation of plant water concentration by the reflectance water index WI (R900/R970). International Journal of Remote Sensing, 18: 2869−2875.

Peters, A.J., Rundquist, D.C., and Wilhite, D.A., (1991), Satellite detection of the geographic core of the 1988 Nebraska drought. Agricultural and Forest Meteorology, 57: 1-3.

Rao, S. Sharma, V. Garg and Venkataraman, G. (2006). "*Soil Moisture Mapping over India using Aqua AMSR-E derived Soil Moisutre Product*", Proceedings of the IEEE International Conference on Geoscience and Remote Sensing Symposium, Denver, USA, 31 July - 4 August 2006, 2999 - 3002

Wang, X., Xie, H., Guan, H., and Zhou, X., (2007), Different responses of MODIS-derived NDVI to root-zone soil moisture in semi-arid and humid regions. Journal of Hydrology, 340: 12– 24.

Wigneron, J.P., Schmugge, T., Chanzy, A., Calvet, J.C. and KERR, Y. (1998). "*Use of passive microwave remote sensing to monitor soil moisture a review*", Agronomie: Agriculture and Environment 18:27-43.

Wilhite D.A., and Buchanan-Smith M. (2005) Drought as Hazard: understanding the natural and social context. In Drought and Water Crises Science, Technology, and Management Issues. Edited by Donald A. Wilhite. Taylor & Francis Group.

Hu Yang, Naimeng Lu, Zhiqiang Ge, et al. “The microwave sensor status and future developing plan of China meteorological satellites”, Proc. SPIE 7452, Earth Observing Systems XIV, 745213 (August 21, 2009); doi:10.1117/12.833758

Jiancheng Shi, Yang Du, Jinyang Du, et al. “Progresses on microwave remote sensing of land surface parameters”, Science China: Earth Sciences, 55(7), 1052-1078, 2012.

J. Shi, L. M. Jiang, L. X. Zhang, et al. "Physically Based Estimation of Bare Surface Soil Moisture with the Passive Radiometers", IEEE Transactions on Geoscience and Remote Sensing, 44(11): 3145- 3153, Nov, 2006.

Jackson T.J., D.M. Le Vine, A.Y. Hsu, et al. “Soil moisture mapping at regional scales using microwave radiometry: the Southern Great Plains Hydrology Experiment”, IEEE Transactions on Geoscience and Remote Sensing, 37(5): 2136-2151, 1999.

Akbari, M., Toomanian, N., Droogers, P., Bastiaanssen, W., and Gieske, A., (2007), Monitoring irrigation performance in Esfahan, Iran, using NOAA

De Ridder, K., (2000), Quantitative estimate of skin soil moisture with the Special Sensor Microwave/Imager. Boundary-Layer Meteorol, 96: 421-432.

Draper, C., Walker, J., Steinle, P., de Jeu, R. and Holmes, T., (2009)."An evaluation of AMSR–E derived soil moisture over Australia", Remote Sensing of Environment, 113 (4), 703-710.

Marshall, G.S., (2005), Drought Detection And Quantification Using Field-Based Spectral Measurements Of Vegetation In Semi-Arid Regions. New Mexico Institute of Mining and Technology Department of Earth and Environmental Science.

Mattia, F., Satalino, G., Pauwels, V.R.N., and Loew A., (2008), Soil moisture retrieval through a merging of multi-temporal L-band SAR data and hydrologic modeling. Hydrology and Earth System Sciences, 5: 3479–3515.

Moran, M.S., Peters-Lidard, C.D., Watts, J.M., and McElroy, S., (2004), Estimating soil moisture at the watershed scale with satellite-based radar and land surface models, Can. J. Remote Sens.

Narasimhan, B., and Srinivasan, R., (2005), Development and evaluation of Soil Moisture Deficit Index (SMDI) and Evapotranspiration Deficit Index (ETDI) for agricultural drought monitoring. Agricultural and Forest Meteorology, 133: 69–88.

Palmer,W.C., (1965), Meteorological Drought. Research Paper No. 45, US Weather Bureau, Washington, DC.

Peñuelas, J., Piñol, J., Ogaya, R., and Filella, I. (1997), Estimation of plant water concentration by the reflectance water index WI (R900/R970). International Journal of Remote Sensing, 18: 2869−2875.

Peters, A.J., Rundquist, D.C., and Wilhite, D.A., (1991), Satellite detection of the geographic core of the 1988 Nebraska drought. Agricultural and Forest Meteorology, 57: 1-3.

Rao, S. Sharma, V. Garg and Venkataraman, G. (2006). "Soil Moisture Mapping over India using Aqua AMSR-E derived Soil Moisutre Product", Proceedings of the IEEE International Conference on Geoscience and Remote Sensing Symposium, Denver, USA, 31 July - 4 August 2006, 2999 - 3002

Wang, X., Xie, H., Guan, H., and Zhou, X., (2007), Different responses of MODIS-derived NDVI to root-zone soil moisture in semi-arid and humid regions. Journal of Hydrology, 340: 12– 24.

Wigneron, J.P., Schmugge, T., Chanzy, A., Calvet, J.C. and KERR, Y. (1998). "Use of passive microwave remote sensing to monitor soil moisture a review", Agronomie: Agriculture and Environment 18:27-43.

Wilhite D.A., and Buchanan-Smith M. (2005) Drought as Hazard: understanding the natural and social context. In Drought and Water Crises Science, Technology, and Management Issues. Edited by Don